RSC Chemical Biology

ROYAL SOCIETY OF CHEMISTRY

PAPER

View Article Online
View Journal | View Issue

Cite this: *RSC Chem. Biol.*, 2024, 5, 776

Probing the metalloproteome: an 8-mercaptoquinoline motif enriches minichromosome maintenance complex components as significant metalloprotein targets in live cells†

Sean M. McKenna,[ab] Bogdan I. Florea,[c] Daniela M. Zisterer,[d] Sander I. van Kasteren[c] and Joanna F. McGouran*[ab]

Affinity-based probes are valuable tools for detecting binding interactions between small molecules and proteins in complex biological environments. Metalloproteins are a class of therapeutically significant biomolecules which bind metal ions as part of key structural or catalytic domains and are compelling targets for study. However, there is currently a limited range of chemical tools suitable for profiling the metalloproteome. Here, we describe the preparation and application of a novel, photoactivatable affinity-based probe for detection of a subset of previously challenging to engage metalloproteins. The probe, bearing an 8-mercaptoquinoline metal chelator, was anticipated to engage several zinc metalloproteins, including the 26S-proteasome subunit Rpn11. Upon translation of the labelling experiment to mammalian cell lysate and live cell experiments, proteomic analysis revealed that several metalloproteins were competitively enriched. The diazirine probe **SMK-24** was found to effectively enrich multiple components of the minichromosome maintenance complex, a zinc metalloprotein assembly with helicase activity essential to DNA replication. Cell cycle analysis experiments revealed that HEK293 cells treated with **SMK-24** experienced stalling in G0/G1 phase, consistent with inactivation of the DNA helicase complex. This work represents an important contribution to the library of cell-permeable chemical tools for studying a collection of metalloproteins for which no previous probe existed.

Received 27th February 2024,
Accepted 18th June 2024

DOI: 10.1039/d4cb00053f

rsc.li/rsc-chembio

Introduction

Affinity-based probes (AfBP) are valuable tools for studying the binding interactions of small molecules in complex and dynamic biological environments.[1,2] AfBPs initially engage target proteins through non-covalent interactions, while the presence of a photoactivatable functional group enables covalent labelling to be initiated through UV irradiation (Fig. 1a).[2,3]

Metal-binding proteins, or metalloproteins, are exciting targets to study using AfBPs, as metal co-factors impart essential structural features or catalytic functions upon biomolecules. However, their non-covalent modes of binding render them difficult targets for profiling studies.[6,7] AfBPs targeting zinc-metalloproteins have previously been made through combination of a zinc-binding group (ZBG) with a photoactivatable moiety and a peptidic or small molecule recognition motif (Fig. 1b and c).[4–9] ZBGs including hydroxamic acids, phosphinic acids, phosphonamides and sulfonamides have been incorporated into AfBPs to target metalloproteins including matrix metalloproteases (MMPs) and carbonic anhydrases (CA).[10–15] However, this existing library of AfBPs employ a tiny fraction of all known ZBGs.[16,17] Furthermore, only a small subset of these AfBPs have been successfully translated to profiling studies in live cells. Therefore, the development of cell-permeable AfBPs incorporating less explored metal-binding groups has major potential to advance the study of the metalloproteome.

Within the ligandable proteome, there remains a large subset of metalloproteins which have thus far eluded detection. These include metalloproteins with key rolls underlying proteostasis, cell cycle regulation and metabolic function.[18–22] We hypothesized that using 8-mercaptoquinole (8MQ) a ZBG

[a] *School of Chemistry, Trinity Biomedical Sciences Institute, Trinity College Dublin, 152-160 Pearse St, Dublin 2, Ireland. E-mail: jmcgoura@tcd.ie*
[b] *Synthesis and Solid State Pharmaceutical Centre (SSPC), Ireland*
[c] *Department of Bioorganic Synthesis, Leiden Institute of Chemistry, Leiden University, Einsteinweg 55, 2333 CC Leiden, The Netherlands*
[d] *School of Biochemistry and Immunology, Trinity Biomedical Sciences Institute, Trinity College Dublin, 152-160 Pearse St, Dublin 2, Ireland*

† Electronic supplementary information (ESI) available. See DOI: https://doi.org/10.1039/d4cb00053f

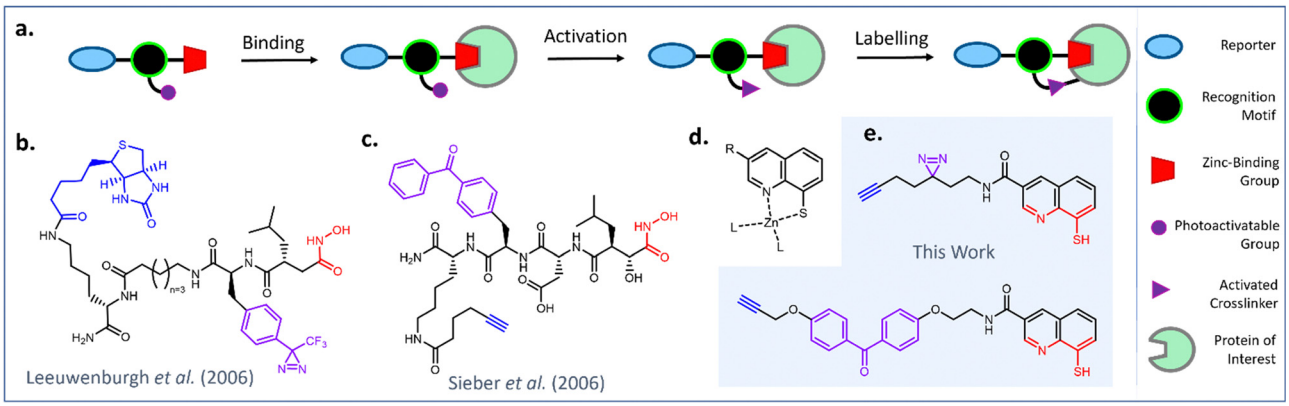

Fig. 1 Design and select examples of AfBPs for profiling the metalloproteome (a) schematic representation of protein labelling with a generic AfBP. (b) Diazirine-functionalized hydroxamic acid probe for MMPs reported by Leeuwenburgh *et al.*[4] (c) Benzophenone-functionalized hydroxamic acid probe for MMP13 reported by Sieber *et al.*[5] (d) Proposed binding mode of 8MQ (e) design of novel AfBPs incorporating an 8MQ metal-binding group.

which has exhibited distinctive metalloenzyme inhibitory activity would allow us to profile an entirely different set of biologically important metalloproteins.[18,23,24] A ZBG library screen by Perez *et al.* had previously discovered that 8MQ effectively inhibited Rpn11, a zinc-dependent member of the JAB1/MPN/Mov34 metalloenzyme (JAMM) family.[18,23] Rpn11 forms part of the 26S proteasome, the multiprotein complex responsible for degradation of damaged and misfolded proteins in eukaryotic cells.[25,26] Inhibition of Rpn11 activity stalls the function of the 26S proteasome, leading to accumulation of redundant proteins and induction of apoptosis.[23,27] Perez *et al.* also identified that 8MQ efficiently inhibited the activity of several members of the JAMM metalloprotease family, while more traditional ZBGs poorly inhibited the activity of these enzymes.[18,23] The screening hit was optimized towards a more potent and selective cell-permeable inhibitor for Rpn11, Capzimin (Fig. S1, ESI†).[23]

In 2019, Hameed *et al.* incorporated 8MQ in a non-covalent probe for detection of JAMM metalloproteases. **Ub-8MQ** (Fig. S2, ESI†) was capable of enriching several overexpressed JAMM deubiquitinases including Rpn11 from cell lysates.[24] The poor cell permeability imparted by the ubiquitin recognition motif prevented profiling studies to be performed in live cells, while the absence of a method for covalent capture impacted the sensitivity of the probe. However, this work still served as an exciting proof of concept and it was recognized that developing a cell-permeable AfBP based upon a minimally functionalized 8MQ scaffold could provide a tool for efficient profiling of several therapeutically significant metalloproteins. We therefore set about designing an AfBP based upon the 8MQ metal-binding motif as a novel profiling tool.

Results and discussion

Probe design and synthesis began with the selection of suitable photoactivatable functional groups. Recent publications describing photoaffinity probes have tended towards the application of diazirines and benzophenones, with alternative moieties such as aryl azides appearing less commonly.[2,28–31] Benzophenones are typically popular due to their relatively long wavelengths for activation, reversibility of solvent quenching, ease of synthesis and stability.[32] However, they also introduce significant steric bulk and high lipophilicity, potentially decreasing the overall selectivity of the probe.[31,33] By contrast, diazirines introduce minimal steric bulk and minimal impact on lipophilicity, but are susceptible to solvent quenching and present a more challenging target for synthesis.[34–36] From a design perspective, the diazirine group appeared favourable for application in this AfBP, as it occupies a similar steric footprint to the reported series of Rpn11 inhibitors.[18] A benzophenone analogue meanwhile was anticipated to be a less favourable binder due to its bulkier size. Both diazirine and benzophenone probes were prepared to compare their labelling properties. A terminal alkyne was used as a minimal reporter handle to enable downstream functionalization with a biotin affinity tag using copper-catalyzed alkyne–azide cycloaddition (CuAAC). Previous studies had utilized 3-carboxamide analogues of 8MQ to introduce a variety of substituents for analysis of structure–activity relationships.[18,23] It was concluded that the photoactivatable group and alkyne reporter handle would also be installed at this position, leaving the remainder of the 8MQ unmodified, thus minimizing the risk of disrupting metal binding.

The JAMM deubiquitinase inhibitor **20** was selected for synthesis as a competitive, non-covalent control. Intermediates **8**, **11** and **18** were each prepared using modified literature conditions (Fig. 2). Amide coupling partners were combined to generate the target probes as disulfide-bridged dimers. The yields for amide coupling reactions using intermediate **18** were low, but consistent with results reported in the literature under these conditions.[18]

Disulfides **19**, **21** and **23** were treated with the reducing agent dithiothreitol (DTT) immediately prior to use to liberate the corresponding thiols **20**, benzophenone **SMK-22** and diazirine **SMK-24** respectively. Diazirine **25** was also prepared as a non-zinc-binding photoaffinity control probe.

To investigate the binding kinetics of the 8MQ motif with zinc(II), a UV-vis titration experiment was performed with diazirine probe **SMK-24** (Fig. 3a). Upon gradual addition of $Zn(ClO_4)_2$ to a solution of **SMK-24**, a significant bathochromic

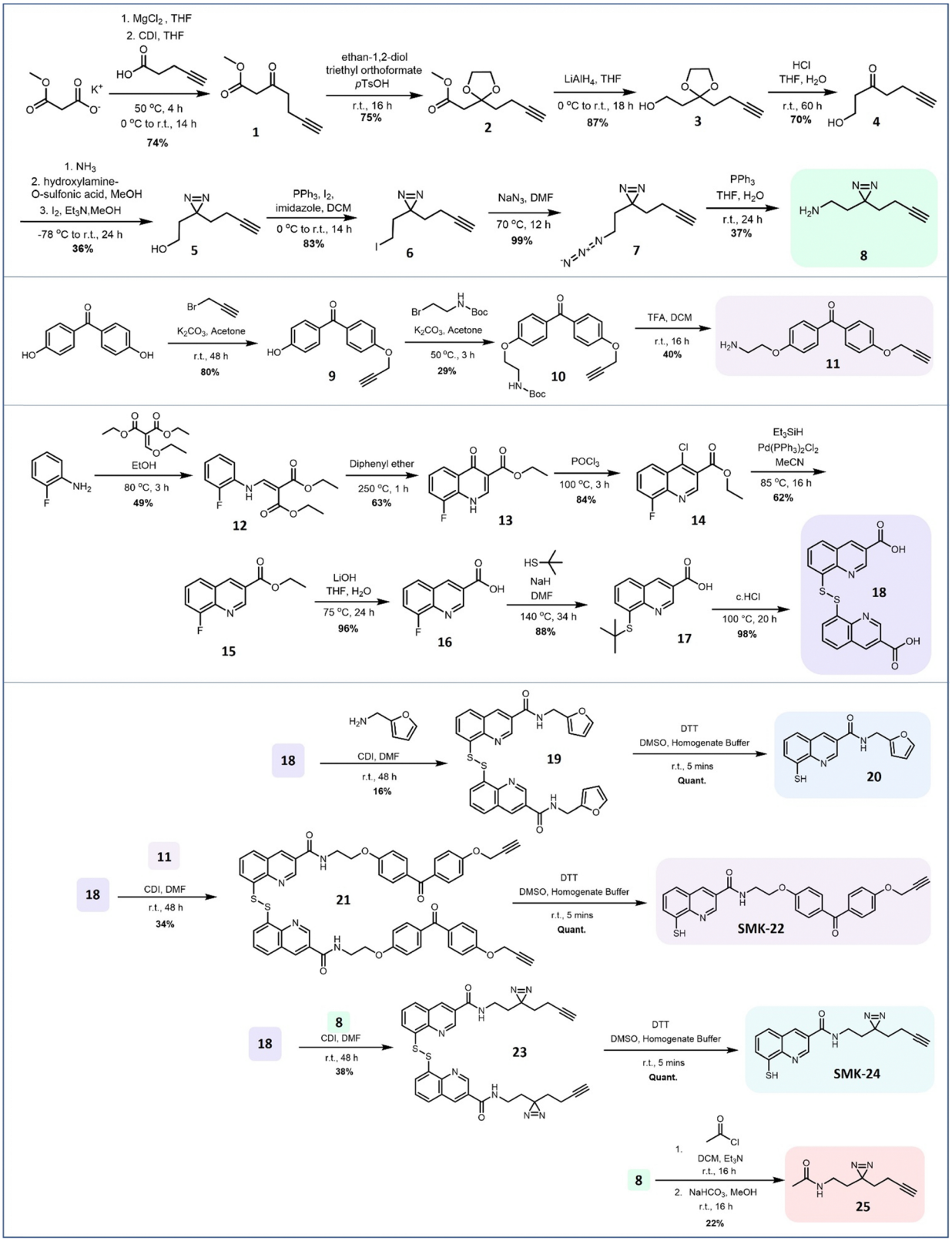

Fig. 2 Synthetic route for the preparation of 8MQ AfBPs **SMK-22** and **SMK-24**. Intermediates **8** and **18** enabled preparation of the 8MQ-bearing **20** and the non-zinc-binding diazirine probe **25** as controls.

shift was observed for absorption maxima at 260 nm and 328 nm to 282 nm and 411 nm respectively. Binding kinetics were modelled in ReactLab and found to be consistent with formation of a Zn(**SMK-24**)$_2$ species with a binding constant of

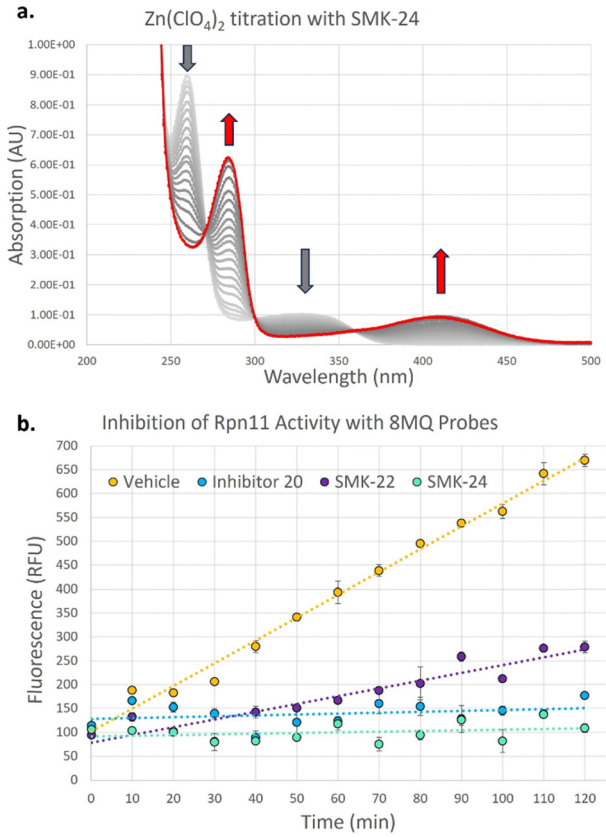

Fig. 3 Investigations into the zinc-binding of the 8MQ AfBPs. (a) Sequential UV-vis absorption measurements (grey) and final spectra recorded (red) of **SMK-24** titrated with $Zn(ClO_4)_2$. (b) Fluorescence assay measuring deubiquitinase activity of recombinant Rpn11/Rpn8 treated with vehicle, 20 μM 8MQ probes **20**, **SMK-22** and **SMK-24**.

$\log k_2$ = 15.2. This result supported the hypothesis that 8MQ acts as a strongly binding bidentate ligand to zinc(II), most similar to hydroxamic acids ($\log k_2$ = 17.5)[37] and sulfonamides ($\log k_2$ = 14.7).[38] By contrast, phosphinic acids ($\log k_2$ = 6.4)[39] and sulfonyl ureas ($\log k_2$ = 3.9)[40,41] exhibit lower association constants as metal chelators, indicating that AfBPs bearing these groups rely upon additional interactions with the protein target to achieve strong binding.

In order to test the synthesized probes on a zinc-metalloenzyme, expression of a recombinant Rpn11/Rpn8 hetereodimer was carried out in BL21 competent *E. coli* cells. Purified Rpn11/Rpn8 was incubated with a fluorogenic substrate, **Ub-AMC** (Fig. S3, ESI†), and an increase in fluorescence over time indicated that the purified Rpn11 enzyme exhibited functional deubiquitinase activity. Treatment of Rpn11/Rpn8 with literature inhibitor **20** resulted in concentration dependent inhibition of enzymatic activity (93% inhibition at 20 μM) (Fig. 3b). Comparable inhibition could be observed with diazirine **SMK-24** (97% inhibition at 20 μM), however benzophenone **SMK-22** exhibited poorer enzyme inhibition (66% inhibition at 20 μM). This indicated that while the incorporation of the aliphatic diazirine and terminal alkyne of **SMK-24** had not significantly perturbed binding to Rpn11 relative to literature inhibitor **20**, the adjustment to a bulkier benzophenone group of **SMK-22** had a detrimental impact on binding.

Next, the capacity for covalent capture of Rpn11 was tested. Recombinant Rpn11/Rpn8 was incubated with the 8MQ AfBPs and subject to UV irradiation. Labelled proteins were conjugated to biotin-PEG4-azide using CuAAC. Proteins were resolved by gel electrophoresis and visualized by western blotting (Fig. 4a) and silver staining (Fig. S4, ESI†). Diazirine probe **SMK-24** was found to successfully label Rpn11 (Fig. 4a, lane 7). Labelling was competitively diminished when an excess of 8MQ-bearing **20** was used (Fig. 4a, lane 4), while minimal labelling could be seen in the absence of UV-irradiation (Fig. 4a, lane 5) and no labelling could be visualized if $CuSO_4$ was not included in the CuAAC reaction mixture (Fig. 4a, lane 6). Incubation with an equivalent concentration of control diazirine **25** showed only trace levels of non-specific labelling (Fig. 4a, lane 3). When Rpn11/Rpn8 was spiked into the protein extract of HEK293 lysate, labelling of the recombinant enzyme could still be observed (Fig. 4a, lane 9). Significantly, diazirine probe **SMK-24** was found to specifically label several other proteins in this complex cell extract mixture, indicating that the probe may have also labelled endogenous cellular metalloproteins. A comparable experiment was performed with benzophenone **SMK-22**, though poorer labelling of Rpn11 was observed and lower specificity labelling was found in HEK293 lysate (Fig. S5, ESI†).

The potential for translation of AfBPs **SMK-22** and **SMK-24** to live cell labelling experiments was now considered. As the 8MQ probes were based on a series on cell-permeable JAMM inhibitors, it was anticipated that they should also permeate live mammalian cells. A parallel artificial membrane permeability assay (PAMPA) was performed to test this hypothesis (Fig. S6, ESI†). Diazirine **SMK-24** effectively permeated the artificial membrane ($\log P_e$ = −5.47) to a comparable degree with the cell active inhibitor **20** ($\log P_e$ = −5.23) and positive permeation control compound carbamazepine ($\log P_e$ = −5.16). However, benzophenone **SMK-22** exhibited poor permeability in this assay ($\log P_e$ = −6.32), comparable to the low permeation control compound furosemide ($\log P_e$ = −6.76). **SMK-22** was also observed to exhibit very poor solubility in aqueous media. Based on its superior performance in experiments to this stage, diazirine **SMK-24** was selected for further study and no further investigations were carried out using benzophenone **SMK-22**.

Anticipating the translatability of **SMK-24** to profiling Rpn11 in live cells, immortalized murine dendritic cells (DC2.4) were selected for initial study. As a well-characterized immune cell line, DC2.4 cells offered the opportunity to study the impact of **SMK-24** on the activity of both the 26S proteasome and immunoproteasome. To examine the permeation of diazirine probe **SMK-24**, a labelling experiment was performed in parallel using both intact and lysed DC2.4 cells. **SMK-24** was incubated with the cell lysate or live DC2.4 cells prior to irradiation. The protein content of labelled live cells was thereafter harvested. All samples were then subject to CuAAC conjugation with biotin-PEG4-azide and proteins were resolved by SDS-PAGE. Western blotting revealed that the major protein bands which were labelled in the lysate samples were also observable in the

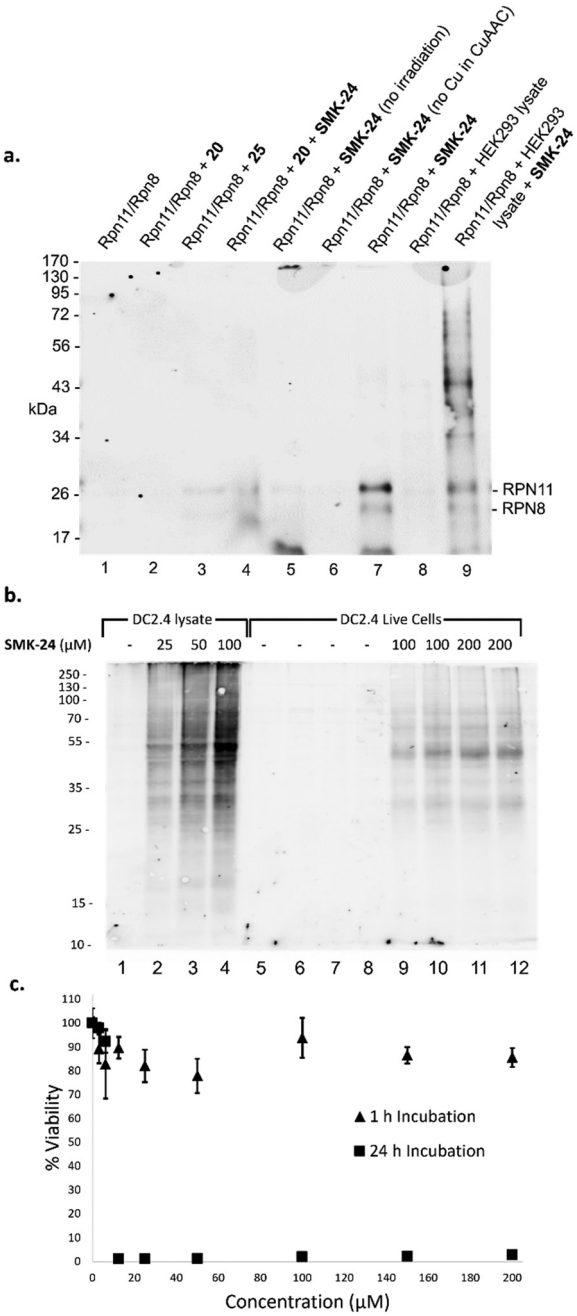

Fig. 4 Application of diazirine probe **SMK-24** in photoaffinity labelling and live cell experiments. (a) Western blot of recombinant Rpn11 labelling with 40 μM **SMK-24** (b) western blot of DC2.4 lysate labelling and live DC2.4 cell labelling with **SMK-24** (0–100 μM and 0–200 μM respectively) (c) MTT cell viability of DC2.4 cells incubated with 0–200 μM **SMK-24** for 1 and 24 h.

live cell samples (Fig. 4b). This supported the viability of **SMK-24** to permeate live cells and to label endogenously expressed proteins without the need to disrupt cell structure.

To assess the effect upon DC2.4 cells of incubation with probe **SMK-24**, an MTT cell viability assay was performed. A concentration range of 0–200 μM **SMK-24** was incubated in DC2.4 cells, with most cells remaining viable even at high probe concentrations following incubation for 1 hour (Fig. 4c). However, when cells were incubated for a longer period of 24 hours, viability dropped close to zero in samples containing >10 μM **SMK-24**. The apparent cytotoxicity of diazirine probe **SMK-24** at concentrations >10 μM with prolonged incubation times guided future protein profiling experiments in live cells to be conducted with an incubation time of just 1 hour.

With diazirine probe **SMK-24** established as a cell-permeable and efficient zinc-binding probe capable of competitively labelling a model zinc metalloenzyme, focus moved to translating this probe towards application in proteomic profiling experiments. Having previously observed that **SMK-24** was capable of labelling discrete protein bands in HEK293 lysate (Fig. 4a), DC2.4 lysate (Fig. 4b) and live cells follow-up studies were performed: proteins labelled with **SMK-24** in HEK293 lysate, DC2.4 lysate and finally in live cell experiments were enriched on avidin beads and subjected to tryptic digest. The resulting peptides were analyzed by LC-MS/MS. Identification, assignment and analysis of constituent peptides was performed using MaxQuant and Perseus.

Proteomics results for diazirine probe **SMK-24** identified several metalloproteins enriched from cell lysate labelling experiments (Fig. 5a and b). Labelling and enrichment experiments were then translated to live DC2.4 cells using an adapted labelling workflow (Fig. 5c) and were subject to proteomic analysis (Fig. 5d). A comparison was made between the cell lysate and live cell labelling experiments and a table of consistently enriched protein hits was compiled (Fig. S7, ESI†). The robustness of metalloprotein hits were examined through further control experiments. Samples treated with both **SMK-24** and 8MQ-bearing **20** in competition were contrasted with samples containing **SMK-24** alone (Fig. 5e). Significantly diminished enrichment of protein hits in competition samples indicated protein binding occurred through engagement of the 8MQ motif. Control experiments with the non-zinc-binding diazirine **25** helped identify proteins enriched through non-specific labelling (Fig. 5f). Those hits which passed these thresholds and could be detected in repeat experiments were considered robust.

The validated metalloprotein hits included *N*-ribosyldihydronicotinamide quinone reductase 2 (NQO2), neudesin neurotrophic factor (NENF), phosphoenolpyruvate carboxykinase 2 (PCK2), calnexin (CANX), acireductone dioxygenase 1 (ADI1) and minichromosome maintenance complex component **6** (MCM6). NQO2, a thioredoxin enzyme dependent upon a zinc co-factor for catalytic activity, plays an important role in stabilizing the tumor suppressor gene p53.[42,43] NENF is an iron-binding protein which promotes cell proliferation in undifferentiated neural progenitor cells and is a prognostic marker in renal cancer cells.[44,45] PCK2 is a mitochondrial kinase dependent upon the binding of a manganese cofactor to enable phosphorylation of oxaloacetate in the citric acid cycle and it's activity has been implicated in chemotherapeutic drug resistance.[21,46] CANX is a calcium and zinc-binding protein which acts as a chaperone in the formation of glycoproteins at the endoplasmic reticulum and is a prognostic marker in colorectal cancer.[47,48] ADI1 is an iron and nickel binding enzyme which functions as a methionine scavenger and exerts tumor

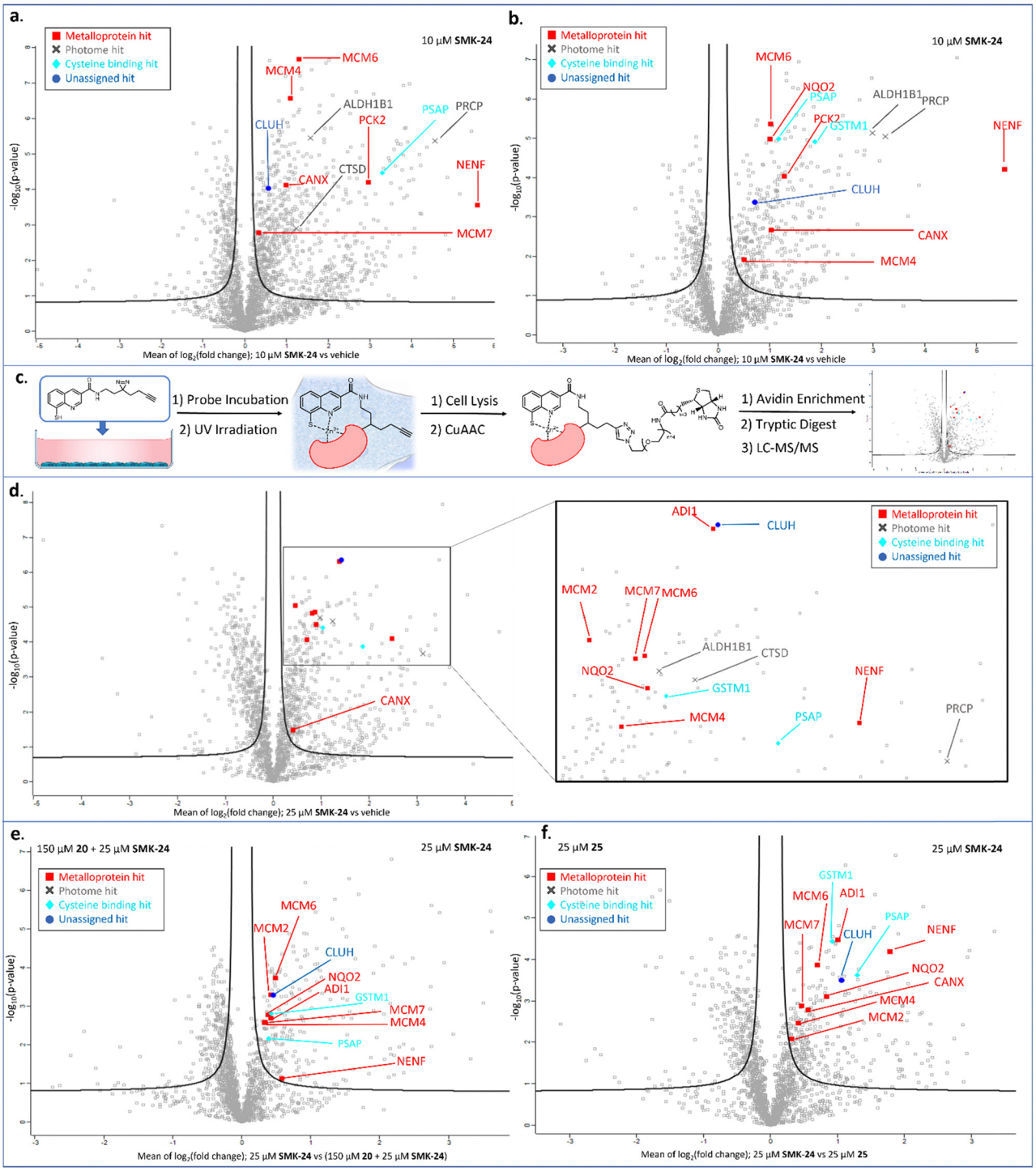

Fig. 5 Identification of proteins enriched through application of AfBP **SMK-24** in lysed and live cell experiments (a) 10 μM **SMK-24** treatment of protein extract from lysed HEK293 cells. (b) 10 μM **SMK-24** treatment of protein extract from lysed DC2.4 cells (c) schematic of live cell labelling workflow with **SMK-24**. (d) 25 μM **SMK-24** treatment in live DC2.4 cells (e) comparison of proteins enriched from 25 μM **SMK-24** treated in live DC2.4 cells (right) *vs.* combination of 150 μM **20** + 25 μM **SMK-24** treated in live DC2.4 cells (left). (f) Comparison of proteins enriched from 25 μM **SMK-24** treated in live DC2.4 cells (right) *vs.* 25 μM diazirine control **25** treated in live DC2.4 cells (left).

suppressor effects in prostate cancer.[49] Excitingly, **SMK-24** was found to enrich a significantly different subset of the metalloproteome than can be profiled using the existing library of metal-binding AfBPs (Fig. 6).[4–8,10–15,50–53] An interesting outcome of the metalloprotein hits discussed above show that 8MQ may also chelate metalloproteins bearing non-zinc metal ion cofactors.

In addition to metal-binding hits, several other commonly enriched proteins were observed in our data sets. A subset of

Publication	Zinc-Binding Group	Covalent Group	Labelling Medium	Labelled Metalloprotein
Chan *et al.*[6] (2004)	Hydroxamic acid	Aryl diazirine, Benzophenone	Purified enzymes	BUD32, DAL1, KAE1, MAS1, MAS2, MMP-9, RPN11 QCR2, Thermolysin, YME1, ZMPSTE24
Saghatelian *et al.*[7] (2004)	Hydroxamic acid	Benzophenone	Purified enzymes	DPP3, LAP, MMP-2, MMP-7, MMP-9, SPG7
Leeuwenburg *et al.*[4] (2006)	Hydroxamic acid	Aryl diazirine	Purified enzyme	ADAM-10
Sieber *et al.*[5] (2006)	Hydroxamic acid	Benzophenone	Cell lysate	ADAM-10, ADAM-17, ADAMTS4, AFG3L2, ALAP, DNPEP, DPP3, ECE, LAP3, LNPEP, LTA4H, MME, MMP-1, MMP-2, MMP-3, MMP-7, MMP-9, MMP-12, NPEPPS, PITRM1, SPG7
Wang *et al.*[8] (2006)	Hydroxamic acid	Benzophenone	Purified enzymes	ALF, Bacterial Collagenase, CA, MMP-3, MMP-7, MMP-14, Thermolysin
David *et al.*[10] (2007)	Phosphinic acid	Aryl azide	Purified enzymes	MMP-2, MMP-3, MMP-8, MMP-9, MMP-11, MMP-12, MMP-13, MMP-14
Dabert-Gay *et al.*[11] (2008)	Phosphinic acid	Aryl azide	Purified enzyme	MMP-12
Qiu *et al.*[50] (2009)	Hydroxamic acid	Aryl diazirine	Purified enzyme	MMP-2
Sakurai *et al.*[52] (2012)	Sulfonamide	Benzophenone	Purified enzyme	CA2
Addy *et al.*[53] (2013)	Sulfonamide	Aryl azide	Purified enzyme	CA2
Nury *et al.*[12] (2013)	Phosphinic acid	Aryl azide	Purified enzymes	MMP-2, MMP-3, MMP-8, MMP-9, MMP-12, MMP-13
Kaminska *et al.*[14] (2021)	Phosphinic acid	Lysine-reactive electrophile	Overexpression live cell model (extracellular targets)	MMP-3, MMP-9, MMP-10, MMP-12, MMP-13
Kennedy *et al.*[15] (2021)	Sulfonyl urea	Aliphatic diazirine	Live cells (including intracellular targets)	CA2, NUCB2, ZMPSTE24
This Work	8-Mercaptoquinoline	Aliphatic diazirine	Live cells (including intracellular targets)	ADO, ADI1, CANX, IDH2, LNPEP, MCM2, MCM4, MCM6, MCM7, NENF, NQO2, NUCB1, NUCB2, PCK2

Fig. 6 Summary of the reported AfBPs for profiling members of the metalloproteome. Key structural motifs and the corresponding metalloprotein(s) labelled are provided. Unique entries are underlined.

these hits including cathepsin D (CTSD), prolylcarboxypeptidase (PRCP) and aldehyde dehydrogenase 1 family member B1 (ALDH1B1) are reported members of the 'photome', a selection of proteins described by Kleiner *et al.* which are readily and non-specifically labelled by diazirine-containing AfBPs.[31] As enrichment of these photome hits was unlikely to be indicative of 8MQ binding, these hits were disregarded. A consistently enriched subset of hits was also found to include cysteine-rich or cysteine-binding proteins such as prosaposin (PSAP), cysteine and glycine rich protein 1 (CSRP1) and glutathione S-transferase mu 1 (GSTM1). Detection of these proteins indicates that **SMK-24** is capable of undergoing *in situ* oxidation to form protein-probe disulfide complexes prior to photoactivation and labelling. Finally, a subset of consistently enriched proteins were identified with no easily assignable binding mode. One such example is clustered mitochondria protein homologue (CLUH), a cytosolic mRNA binding protein, which was consistently and competitively enriched in cell lysate and live cell experiments with diazirine probe **SMK-24** (Fig. 5d–f and Fig. S8, S9, ESI†).

To our knowledge, there has been no report of CLUH binding metal ion co-factors. However, our results suggest that CLUH may be capable of binding a metal ion co-factor or associating with a secondary metalloprotein in the cellular environment.

Despite labelling several metalloproteins, we were surprised to discover that **SMK-24** had not enriched endogenously expressed Rpn11 from the extracts of either HEK293 or DC2.4 cells. Increasing the loading of **SMK-24** to high concentrations ($\leq$200 μM) was not found to result in Rpn11 enrichment. A possible explanation for this finding is that **SMK-24** may have bound effectively to the purified recombinant Rpn11/Rpn8 heterodimer, but not to endogenous Rpn11 in the greater structure of the 26S proteasome. Alternatively, the selection of the diazirine photoactivatable group in this probe may have been suboptimal for Rpn11 labelling.

The metalloprotein hit most consistently enriched by diazirine probe **SMK-24** in lysate and live cell labelling experiments was minichromosome maintenance complex component **6** (MCM6). MCM6 is a nucleosomal protein which forms part of a hexameric DNA helicase complex in once per cell-cycle DNA replication.[54,55] The complex is formed through interaction of MCM components **2–7** (MCM2–7) and is recruited to DNA replication origins by CDT1 and CDC6.[56,57] In addition to MCM6 enrichment, MCM4 and MCM7 were also labelled in lysate experiments (Fig. 5a and b). The MCM components share several common structural motifs, including an N-terminal zinc finger domain which is understood to play a key role in hexamer formation and binding of DNA for helicase activity.[57,58] Given that diazirine probe **SMK-24** enriched MCM6 in a competitive manner with 8MQ-bearing **20**, and was not enriched by non-zinc-binding control **25**, it was rationalized that **SMK-24** was binding MCM6 *via* the zinc-finger domain. MCM6 overexpression has been found to be an adverse prognostic marker in several cancer types, including lung cancer, breast cancer, glioma, lymphoma and oesophageal squamous cell

carcinoma.[55,59–61] MCM4 and MCM7 overexpression has been found to be adversely prognostic in cases of oesophageal carcinoma and squamous cell carcinoma.[61–63] The overexpression of MCM2 has been associated with oral squamous cell carcinoma and cervical carcinoma, while MCM3 and MCM5 have been found as biomarkers of dysplastic oral lesions and renal cell carcinoma respectively.[19,20,64] An AfBP for detection of MCM components could therefore prove to be a valuable tool in diagnostics and research. As a result, focus moved towards establishing the viability of **SMK-24** as a tool for detection of MCM components.

We were delighted to discover that several MCM components, including MCM2, MCM4, MCM6 and MCM7 could be successfully enriched through application of diazirine probe **SMK-24** in live DC2.4 cell labelling experiments (Fig. 5d). Labelling of these components was found to be competitive with 8MQ-bearing **20** (Fig. 5e), while enrichment was observed above the non-zinc-binding diazirine **25** (Fig. 5f and Fig. S9, ESI†). A follow-up live cell labelling experiment was performed in primary bone marrow derived dendritic cells (BMDC) (Fig. S11, ESI†), where MCM6 was enriched as the only detectable MCM component.

It was recognized that in binding MCM components *via* a functionally crucial zinc-finger domain, diazirine probe **SMK-24** may disrupt the formation or activity of the MCM helicase complex. This would affect the cell's ability to duplicate DNA, hence stalling its transition from the growth (G1) phase to the DNA synthesis (S) phase of the cell cycle. To test whether treatment with **SMK-24** caused cells to stall in the quiescent (G0) or G1 phase, a study was performed where HEK293 cells were incubated with **SMK-24** for 1–10 h, after which cells were fixed and treated with the DNA stain propidium iodide.[65] The DNA content of the cells was analyzed using flow cytometry (Fig. 7a and Fig. S12, ESI†).

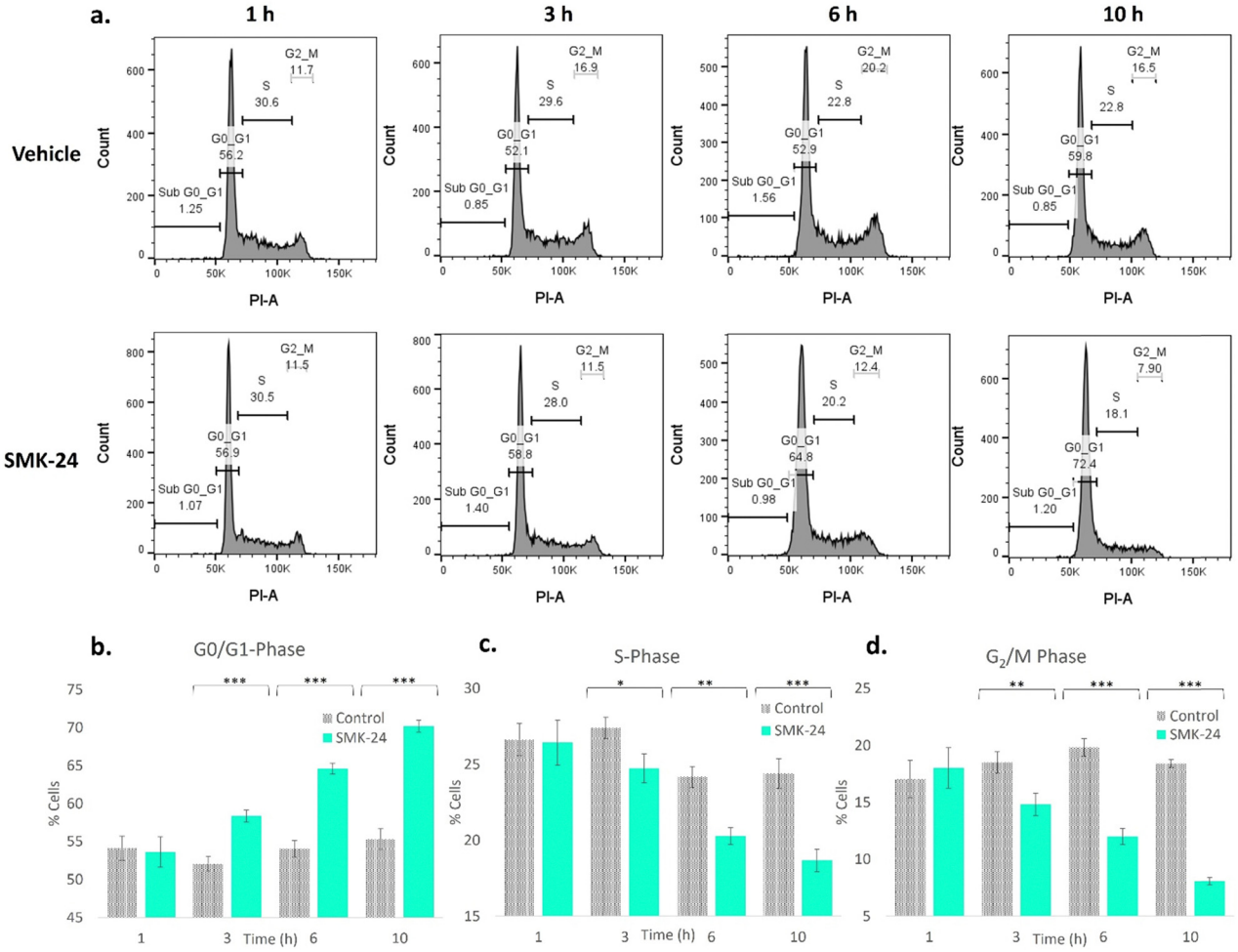

Fig. 7 Effects of diazirine probe **SMK-24** on the cell cycle of HEK293 cells. Cells were treated with vehicle (0.1% DMSO, 150 μM DTT) or 25 μM **SMK-24** in DMEM growth medium for 1–10 h and thereafter fixed and stained with propidium iodide. (a) Stained cells were analysed by flow cytometry. Cell cycle analysis was performed on histograms of gated counts per DNA area (FL2-A). Plots are representative examples of results from three separate experiments. Number of cells in sub-G0/G1-phase, (b) G0/G1-phase, (c) S-phase and (d) G2/M phase was determined using FlowJo software. Values represent the mean and standard error for three separate experiments. Statistical analysis was performed using one-way ANOVA followed by Dunnett's multiple comparison test (*$p < 0.05$; **$p < 0.01$; ***$p < 0.001$). Treatment of cells with **SMK-24** resulted in significant population increase in G0/G1 phase, with concomitant population decrease in S phase and in G2/M phase from 3–10 h. Results are representative of three separate experiments where samples were prepared in triplicate per condition.

Analysis of cells treated with diazirine probe **SMK-24** revealed significant changes in cell cycle population over the duration of the experiment. The relative population of cells in G0/G1-phase increased over time (Fig. 7b), while the population of cells in S-phase (Fig. 7c) and growth 2 (G2) phase and mitosis (M) (Fig. 7d) decreased. This result is consistent with disruption or inactivation of the MCM helicase complex, resulting in greater numbers of cells stalling in G0/G1 phase. This effect may be augmented by cellular stresses resulting from off-target engagement of **SMK-24**, as well as zinc scavenging effects which may disrupt cellular signalling and cause a greater proportion of cells to enter the G0 quiescence state. No significant change was observed in the population of apoptotic cells in the sub-G0/G1 population over the course of this experiment, indicating that population changes were not significantly driven by apoptotic cell death.

The MCM components are perhaps the most significant metalloproteins to be detected using probe **SMK-24**. While 8MQ-containing compounds are known to exhibit off-target activity, the identification of several binding partners implicated in key DNA replication machinery is potentially significant. These results would justify further investigations to detect whether other 8MQ-containing compounds exert similar effects on the cell cycle. This may reveal an exciting opportunity for future research into a diagnostically significant class of metalloproteins.

Conclusions

We have developed a photoactivatable affinity-based probe for profiling a range of metalloproteins in live cell experiments. Diazirine probe **SMK-24** was demonstrated to successfully labelled Rpn11 in a simple model system, but proved not to be translatable to detection of the endogenously expressed native enzyme. Instead, several therapeutically significant metalloproteins were successfully enriched from lysate and live cell labelling experiments and identified using proteomics. We discovered several components of the minichromosome maintenance complex as novel metalloprotein binding partners of **SMK-24**. In particular, we recognized MCM6, an adverse prognostic biomarker in several cancer variants, to be consistently and sensitively enriched with **SMK-24** in the mammalian cell lines tested. Finally, we demonstrated that treatment of **SMK-24** in HEK293 cells resulted in significant changes in cell cycle population, consistent with inactivation of the MCM helicase complex. We anticipate **SMK-24** to be an important tool in the study of several therapeutically significant metalloproteins.

Author contributions

Probe design was performed by S. M. M. and J. F. M. Experiment design was performed by S. M. M., J. F. M., S. I. V. K., B. I. F. and D. M. Z. All practical chemistry and biology was performed by S. M. M. LC-MS/MS data acquisition was performed by B. I. F. Data processing and analysis was performed by S. M. M. The manuscript was written by S. M. M. and J. F. M.

Data availability

Characterisation data for all compounds is available in the ESI† as are further supporting experimental data referenced in the manuscript. Chemical and biochemical experimental methods are also included as are NMR spectra of the probe disulfide precursor compounds. Proteomics data is available through the PRIDE partner repository using the identifier: PXD052663.

Conflicts of interest

There are no conflicts to declare.

Acknowledgements

This publication was supported by the Synthesis and Solid State Pharmaceutical Centre (SSPC), funded by Science Foundation Ireland (SFI) Grant no. 12/RC/2275_P2 (J. F. M.), Trinity College Dublin (J. F. M.), European Molecular Biology Organisation, Scientific Exchange Grant no. 9879 (S. M. M.) and ERC CoG KineTic grant number 865175 (S. I. V. K.). We wish to thank Professor Andreas Martin of UC Berkley for generously permitting use of the plasmid for Rpn11/Rpn8 expression and Dr Dharjath Hameed of Leiden University Medical Center, Leiden University for supplying the plasmid and providing valuable guidance on expression and purification. We also wish to thank Dr John O'Brien and Dr Gary Hessman in Trinity College Dublin School of Chemistry for support in compound characterization and to Dr Barry Moran in Trinity College Dublin School of Biochemistry and Immunology for support in flow cytometry. Finally, we wish to thank Dr Amber Barendrecht, Constant Tellinga, Dr Nina Ligthart, Thijmen Mostert and Dr Tyrza van Leeuwen of Leiden Institute of Chemistry, Leiden University for kindly donating cells for lysate labelling experiments. The mass spectrometry proteomics data have been deposited to the ProteomeXchange Consortium *via* the PRIDE partner repository with the dataset identifier PXD052663.[66]

Notes and references

1 B. F. Cravatt, A. T. Wright and J. W. Kozarich, *Annu. Rev. Biochem.*, 2008, **77**, 383–414.
2 S. M. McKenna, E. M. Fay and J. F. McGouran, *ACS Chem. Biol.*, 2021, **16**, 2719–2730.
3 H. Fang, B. Peng, S. Y. Ong, Q. Wu, L. Li and S. Q. Yao, *Chem. Sci.*, 2021, **12**, 8288–8310.
4 M. A. Leeuwenburgh, P. P. Geurink, T. Klein, H. F. Kauffman, G. A. Van Der Marel, R. Bischoff and H. S. Overkleeft, *Org. Lett.*, 2006, **8**, 1705–1708.
5 S. A. Sieber, S. Niessen, H. S. Hoover and B. F. Cravatt, *Nat. Chem. Biol.*, 2006, **2**, 274–281.
6 E. W. S. Chan, S. Chattopadhaya, R. C. Panicker, X. Huang and S. Q. Yao, *J. Am. Chem. Soc.*, 2004, **126**, 14435–14446.
7 A. Saghatelian, N. Jessani, A. Joseph, M. Humphrey and B. F. Cravatt, *Proc. Natl. Acad. Sci. U. S. A.*, 2004, **101**, 10000–10005.

8 J. Wang, M. Uttamchandani, J. Li, M. Hu and S. Q. Yao, *Chem. Commun.*, 2006, 3783–3785.
9 R. Nakai, C. M. Salisbury, H. Rosen and B. F. Cravatt, *Bioorg. Med. Chem.*, 2009, **17**, 1101–1108.
10 A. David, D. Steer, S. Bregant, L. Devel, A. Makaritis, F. Beau, A. Yiotakis and V. Dive, *Angew. Chem., Int. Ed.*, 2007, **46**, 3275–3277.
11 A. S. Dabert-Gay, B. Czarny, L. Devel, F. Beau, E. Lajeunesse, S. Bregant, R. Thai, A. Yiotakis and V. Dive, *J. Biol. Chem.*, 2008, **283**, 31058–31067.
12 C. Nury, B. Czarny, E. Cassar-Lajeunesse, D. Georgiadis, S. Bregant and V. Dive, *ChemBioChem*, 2013, **14**, 107–114.
13 K. Teruya, K. F. Tonissen and S. A. Poulsen, *MedChemComm*, 2016, **7**, 2045–2062.
14 M. Kaminska, P. Bruyat, C. Malgorn, M. Doladilhe, E. Cassar-Lajeunesse, C. Fruchart Gaillard, M. De Souza, F. Beau, R. Thai, I. Correia, A. Galat, D. Georgiadis, O. Lequin, V. Dive, S. Bregant and L. Devel, *Angew. Chem.*, 2021, **133**, 18420–18427.
15 C. R. Kennedy, A. Goya Grocin, T. Kovačič, R. Singh, J. A. Ward, A. R. Shenoy and E. W. Tate, *ACS Chem. Biol.*, 2021, **16**, 982–990.
16 A. Agrawal, S. L. Johnson, J. A. Jacobsen, M. T. Miller, L. H. Chen, M. Pellecchia and S. M. Cohen, *ChemMedChem*, 2010, **5**, 195–199.
17 J. A. Jacobsen, J. L. Fullagar, M. T. Miller and S. M. Cohen, *J. Med. Chem.*, 2011, **54**, 591–602.
18 C. Perez, J. Li, F. Parlati, M. Rouffet, M. Yuyong, A. L. Mackinnon, T. F. Chou, R. J. Deshaies and S. M. Cohen, *J. Med. Chem.*, 2017, **60**, 1343–1361.
19 H. Zhong, B. Chen, H. Neves, J. Xing, Y. Ye, Y. Lin, G. Zhuang, S. D. Zhang, J. Huang and H. F. Kwok, *Cancer Manag. Res.*, 2017, **9**, 637–647.
20 Y. Li, J. Zou, Q. Zhang, F. Quan, L. Cao, X. Zhang, J. Liu and D. Wu, *Front. Oncol.*, 2021, **11**, 1–17.
21 Z. Jing, J. Gao, J. Li, F. Niu, L. Tian, P. Nan, Y. Sun, X. Xie, Y. Zhu, Y. Zhao, F. Liu, L. Zhou, Y. Sun and X. Zhao, *Cancer Lett.*, 2021, **519**, 46–62.
22 Y. De Chu, H. Y. Lai, L. M. Pai, Y. H. Huang, Y. H. Lin, K. H. Liang and C. T. Yeh, *Cell Death Dis.*, 2019, **10**, 240.
23 J. Li, T. Yakushi, F. Parlati, A. L. MacKinnon, C. Perez, Y. Ma, K. P. Carter, S. Colayco, G. Magnuson, B. Brown, K. Nguyen, S. Vasile, E. Suyama, L. H. Smith, E. Sergienko, A. B. Pinkerton, T. D. Y. Chung, A. E. Palmer, I. Pass, S. Hess, S. M. Cohen and R. J. Deshaies, *Nat. Chem. Biol.*, 2017, **13**, 486–493.
24 D. S. Hameed, A. Sapmaz, L. Burggraaff, A. Amore, C. J. Slingerland, G. J. P. van Westen and H. Ovaa, *Angew. Chem., Int. Ed.*, 2019, **58**, 14477–14482.
25 N. C. Taylor and J. F. McGouran, *Front. Chem.*, 2020, **7**, 914.
26 T. E. T. Mevissen and D. Komander, *Annu. Rev. Biochem.*, 2017, **86**, 159–192.
27 H. A. Bustamante, N. Albornoz, E. Morselli, A. Soza and P. V. Burgos, *Cell. Signal.*, 2023, **101**, 1–7.
28 J. Wang, Q. Chen, Y. Shan, X. Pan and J. Zhang, *Trends Anal. Chem.*, 2019, **115**, 110–120.
29 D. P. Murale, S. C. Hong, M. M. Haque and J. S. Lee, *Proteome Sci.*, 2017, **15**, 1–34.
30 J. R. Hill and A. A. B. Robertson, *J. Med. Chem.*, 2018, **61**, 6945–6963.
31 P. Kleiner, W. Heydenreuter, M. Stahl, V. S. Korotkov and S. A. Sieber, *Angew. Chem., Int. Ed.*, 2017, **56**, 1396–1401.
32 J. P. Holland, M. Gut, S. Klingler, R. Fay and A. Guillou, *Chem. - Eur. J.*, 2020, **26**, 33–48.
33 L. L. Punzalan, L. Jiang, D. Mao, A. Das Mahapatra, S. Sato, Y. Takemoto, M. Tsujimura, K. Kusamori, M. Nishikawa, L. Zhou and M. Uesugi, *Cell Chem. Biol.*, 2020, **27**, 708–718.
34 L. Dubinsky, B. P. Krom and M. M. Meijler, *Bioorg. Med. Chem.*, 2012, **20**, 554–570.
35 A. V. West, G. Muncipinto, H. Y. Wu, A. C. Huang, M. T. Labenski, L. H. Jones and C. M. Woo, *J. Am. Chem. Soc.*, 2021, **143**, 6691–6700.
36 H. Park, J. Y. Koo, Y. V. V. Srikanth, S. Oh, J. Lee, J. Park and S. B. Park, *Chem. Commun.*, 2016, **52**, 5828–5831.
37 P. Buglyó, E. M. Nagy, E. Farkas, I. Sóvágó, D. Sanna and G. Micera, *Polyhedron*, 2007, **26**, 1625–1633.
38 T. Koike, E. Kimura, I. Nakamura, Y. Hashimoto and M. Shiro, *J. Am. Chem. Soc.*, 1992, **114**, 7338–7345.
39 M. Lukáš, M. Kývala, P. Hermann, I. Lukeš, D. Sanna and G. Micera, *J. Chem. Soc. Dalt. Trans.*, 2001, 2850–2857.
40 B. Y. Guo, W. L. Wei and J. M. Lin, *J. Chromatogr. Sci.*, 2009, **47**, 116–120.
41 P. A. Shah, J. V. Shah, M. Sanyal and P. S. Shrivastav, *Int. J. Pharm. Pharm. Sci.*, 2015, **7**, 105–111.
42 K. K. K. Leung and B. H. Shilton, *J. Biol. Chem.*, 2013, **288**, 11242–11251.
43 Z. Lin, X. Wang, K. A. Bustin, K. Shishikura, N. R. McKnight, L. He, R. M. Suciu, K. Hu, X. Han, M. Ahmadi, E. J. Olson, W. H. Parsons and M. L. Matthews, *ACS Cent. Sci.*, 2021, **7**, 1524–1534.
44 H. Ohta, I. Kimura, M. Konishi and N. Itoh, *Front. Mol. Biosci.*, 2015, **2**, 1–5.
45 I. Kimura, Y. Nakayama, Y. Zhao, M. Konishi and N. Itoh, *Front. Neurosci.*, 2013, **7**, 1–5.
46 M. Escós, P. Latorre, J. Hidalgo, R. Hurtado-Guerrero, J. A. Carrodeguas and P. López-Buesa, *Biochem. Biophys. Rep.*, 2016, **7**, 124–129.
47 D. B. Williams, *J. Cell Sci.*, 2006, **119**, 615–623.
48 D. Ryan, S. Carberry, Á. C. Murphy, A. U. Lindner, J. Fay, S. Hector, N. McCawley, O. Bacon, C. G. Concannon, E. W. Kay, D. A. McNamara and J. H. M. Prehn, *J. Transl. Med.*, 2016, **14**, 1–10.
49 S. W. Oram, J. Ai, G. M. Pagani, M. R. Hitchens, J. A. Stern, S. Eggener, M. Pins, W. Xiao, X. Cai, R. Haleem, F. Jiang, T. C. Pochapsky, L. Hedstrom and Z. Wang, *Neoplasia*, 2007, **9**, 643–651.
50 W. Qiu, J. Xu, X. Li, L. Zhong, J. Li, J. Li and F. Nan, *Chin. J. Chem.*, 2009, **27**, 825–833.
51 P. P. Geurink, T. Klein, L. Prèly, K. Paal, M. A. Leeuwenburgh, G. A. Van Der Marel, H. F. Kauffman, H. S. Overkleeft and R. Bischoff, *Eur. J. Org. Chem.*, 2010, 2100–2112.
52 K. Sakurai, M. Tawa, A. Okada, R. Yamada, N. Sato, M. Inahara and M. Inoue, *Chem. – Asian J.*, 2012, **7**, 1567–1571.

53 P. S. Addy, B. Saha, N. D. P. Singh, A. K. Das, J. T. Bush, C. Lejeune, C. J. Schofield and A. Basak, *Chem. Commun.*, 2013, **49**, 1930–1932.
54 N. Tuteja and R. Tuteja, *Eur. J. Biochem.*, 2004, **271**, 1835–1848.
55 L. Cheng, Z. Tan, Z. Huang, Y. Pan, W. Zhang and J. Wang, *Med. Sci. Monit.*, 2020, **26**, 1–15.
56 Z. Wei, C. Liu, X. Wu, N. Xu, B. Zhou, C. Liang and G. Zhu, *J. Biol. Chem.*, 2010, **285**, 12469–12473.
57 Y. Zhai, E. Cheng, H. Wu, N. Li, P. Y. K. Yung, N. Gao and B. K. Tye, *Nat. Struct. Mol. Biol.*, 2017, **24**, 300–308.
58 Z. You, Y. Ishimi, H. Masai and F. Hanaoka, *J. Biol. Chem.*, 2002, **277**, 42471–42479.
59 T. Zeng, Y. Guan, Y. Kun Li, Q. Wu, X. Jun Tang, X. Zeng, H. Ling and J. Zou, *Clin. Chim. Acta*, 2021, **517**, 92–98.
60 Y. Gu, X. Hu, X. Liu, C. Cheng, K. Chen, Y. Wu and Z. Wu, *BMC Cancer*, 2021, **21**, 1–14.
61 T. Cao, S. J. Yi, L. X. Wang, J. X. Zhao, J. Xiao, N. Xie, Z. Zeng, Q. Han, H. O. Tang, Y. K. Li, J. Zou and Q. Wu, *BioMed*, 2020, 3574261.
62 C. J. Feng, H. J. Li, J. N. Li, Y. J. Lu and G. Q. Liao, *Anticancer Res.*, 2008, **28**, 3763–3769.
63 S. Yang, Y. Yuan, W. Ren, H. Wang, Z. Zhao, H. Zhao, Q. Zhao, X. Chen, X. Jiang and L. Zhang, *Front. Oncol.*, 2022, **12**, 1–23.
64 A. G. Lameira, F. S. C. Pontes, D. M. Guimarães, A. C. G. Alves, A. S. de Jesus, H. A. R. Pontes, D. dos and S. Pinto, *J. Oral Pathol. Med.*, 2014, **43**, 427–434.
65 M. J. Meegan, S. Nathwani, B. Twamley, D. M. Zisterer and N. M. O'Boyle, *Eur. J. Med. Chem.*, 2017, **125**, 453–463.
66 Y. Perez-Riverol, J. Bai, C. Bandla, D. Garcia-Seisdedos, S. Hewapathirana, S. Kamatchinathan, D. J. Kundu, A. Prakash, A. Frericks-Zipper, M. Eisenacher, M. Walzer, S. Wang, A. Brazma and J. A. Vizcaíno, *Nucleic Acids Res.*, 2021, **50**, D543–D552.